Virology 429 (2012) 124–135

Contents lists available at SciVerse ScienceDirect

Virology

journal homepage: www.elsevier.com/locate/yviro

Herpes simplex virus 1 induces *de novo* phospholipid synthesis

Esther Sutter [a], Anna Paula de Oliveira [b], Kurt Tobler [b], Elisabeth M. Schraner [a], Sabrina Sonda [c,1], Andres Kaech [d], Miriam S. Lucas [e], Mathias Ackermann [b], Peter Wild [a,*]

[a] *Electron Microscopy, Institute of Veterinary Anatomy, University of Zürich, Switzerland*
[b] *Electron microscopy, Institute of Virology, University of Zürich, Switzerland*
[c] *Institute of Parasitology, University of Zürich, Switzerland*
[d] *Center for Microscopy and Image Analysis, University of Zürich, Switzerland*
[e] *Electron Microscopy ETH Zürich (EMEZ), Swiss Federal Institute of Technology, Zürich, Switzerland*

ARTICLE INFO

Article history:
Received 1 December 2011
Accepted 10 April 2012
Available online 5 May 2012

Keywords:
Herpes virus
Intracellular traffic
Nuclear membranes
Golgi membranes
Phospholipid synthesis
SEM
TEM
Morphometry

ABSTRACT

Herpes simplex virus type 1 capsids bud at nuclear membranes and Golgi membranes acquiring an envelope composed of phospholipids. Hence, we measured incorporation of phospholipid precursors into these membranes, and quantified changes in size of cellular compartments by morphometric analysis. Incorporation of [^{3}H]-choline into both nuclear and cytoplasmic membranes was significantly enhanced upon infection. [^{3}H]-choline was also part of isolated virions even grown in the presence of brefeldin A. Nuclei expanded early in infection. The Golgi complex and vacuoles increased substantially whereas the endoplasmic reticulum enlarged only temporarily. The data suggest that HSV-1 stimulates phospholipid synthesis, and that *de novo* synthesized phospholipids are inserted into nuclear and cytoplasmic membranes to i) maintain membrane integrity in the course of nuclear and cellular expansion, ii) to supply membrane constituents for envelopment of capsids by budding at nuclear membranes and Golgi membranes, and iii) to provide membranes for formation of transport vacuoles.

Introduction

Herpes simplex virus type 1 (HSV-1) is composed of 4 morphological distinct substructures: the core containing the viral DNA, the icosahedral capsid built of 162 capsomers, the tegument surrounding the capsid, and the viral envelope with embedded glycoproteins (Roizman and Knipe, 2001). The way of assembly of these different structures is highly complex (Roizman, Knipe, and Whiley, 2007). Capsids are assembled within nuclei and then transported to the nuclear periphery. There they bud at the inner nuclear membrane (INM) acquiring the viral envelope and tegument (Granzow, 2001; Leuzinger et al., 2005). The result is a fully enveloped virion within the perinuclear space (PNS) that is delineated by the INM and outer nuclear membrane (ONM). The ONM continues into the INM at the sites of thousands of nuclear pores (Maul, 1977; Wild et al., 2009) which are occupied by the nuclear pore complexes (Goldberg and Allen, 1995; Lim and Fahrenkrog, 2006). The ONM also continues into membranes of the rough endoplasmic reticulum (RER) and is, like the RER, studded with ribosomes. Capsids have been reported to overcome the nucleocytoplasmic barrier after impairment of nuclear membranes (Borchers and Oezel, 1993; Klupp et al., 2011) which have been suggested to result in dilation of nuclear pores (Wild et al., 2009).

Transportation of virions out of the PNS is controversially discussed (Roizman et al., 2007). Currently, the most favored idea is that perinuclear virions are de-enveloped by fusion of the viral envelope with the ONM releasing tegument and capsids into the cytoplasmic matrix as suggested for the first time in 1969 (Stackpole, 1969) to explain the presence of naked capsids within the cytoplasmic matrix. These capsids need then to be re-enveloped by budding at the trans-Golgi network to become infective (Skepper et al., 2001). During de-envelopment the viral envelope derived by budding from the INM is inserted into the ONM. Recently, it was shown that dozens of capsids can bud simultaneously at the INM (Wild et al., 2009). The question thus arises about the origin of lipids necessary for envelopment at the INM.

The Golgi complex plays a crucial role in herpes virus envelopment and in formation of transport vacuoles. Capsids are assumed to bud at vesicles of the trans Golgi network concomitantly forming the viral envelope and the transport vacuoles (Mettenleiter, 2004; Mettenleiter et al., 2006), a process referred to as wrapping. Alternatively, capsids were shown to bud into large vacuoles (Homman-Loudiyi et al., 2003; Leuzinger et al., 2005) and at membranes of any site of the Golgi complex (Leuzinger et al., 2005; Wild et al., 2002). Furthermore, enveloped virions were

* Corresponding author. Fax: +41 1 635 89 11.
E-mail address: pewild@access.uzh.ch (P. Wild).
[1] Current address: Swiss Hepato-Pancreato-Biliary Center, Department of Visceral and Transplantation Surgery, University Hospital, Zürich

0042-6822/$ - see front matter © 2012 Elsevier Inc. All rights reserved.
http://dx.doi.org/10.1016/j.virol.2012.04.004

demonstrated within lateral cisternae of the Golgi complex (Leuzinger et al., 2005; Torrisi et al., 1992; Wild et al., 2002). Membranes of lateral cisternae containing virions showed indications for fission which results in formation of transport vacuoles (Palade, 1975). Wrapping, budding of capsids into vacuoles, and formation of transport vacuoles by fission require membranes that need to be provided either by recruitment from other cellular sites, e.g. by recycling from the plasma membrane via endocytosis as shown in secretory cells (Orci et al., 1981) or by *de novo* synthesis.

Although envelopment plays an essential role in formation of infective HSV-1 virus particles mechanisms of budding and fusion as well as origin and metabolism of lipids are poorly investigated. One of the first studies suggested that [^{3}H]-choline labeled lipids become part of the viral envelope during budding at nuclear membranes (Asher et al., 1969). Incorporation of [^{32}P]-phosphate into sphingomyelin was increased in HSV-1 infected skin fibroblasts whereas incorporation into other phospholipids was unaltered. The distribution of [^{32}P]-phosphate labeled phospholipids in the viral envelop was shown to be identical to that of cellular membranes (Steinhart et al., 1981). Lipid analysis revealed that the lipid composition of the envelope differs from that of host cell nuclear membranes but was not identical to that of Golgi membranes (van Genderen et al., 1995).

The high demand for membranes used for herpes virus envelopment per se and for formation of transport vacuoles prompted us to investigate cell membrane alterations during HSV-1 infection by measuring incorporation of [^{3}H]-choline into nuclear membranes and cytoplasmic membranes, and by quantifying cellular compartments by transmission electron microscopic (TEM) morphometry. To address the budding activity at the inner nuclear membrane, we also imaged the nuclear surface by high resolution scanning electron microscopy (Cryo-FESEM). We show that [^{3}H]-choline incorporation into both nuclear and cytoplasmic membranes is significantly enhanced during HSV-1 infection suggesting *de novo* phospholipid synthesis to provide membranes needed for maintenance of cellular compartments and for viral envelopment.

Results

Incorporation of [^{3}H]-choline into nuclear and cytoplasmic membranes increases after HSV-1 infection

Electron microscopy confirmed that the procedure for isolation of nuclei yielded a nuclear fraction consisting merely of nuclei surrounded by nuclear membranes and some cytoplasmic membranes (Fig. 1A) whereas the cytoplasmic fraction contained exclusively membranous compartments (Fig. 1B). The procedure applied for virus purification yielded mainly intact virions and some contamination with membranous material (Fig. 1C). Phospholipid composition varies throughout the cell. The major component in all membranes is phosphatidylcholine (van Meer et al., 2008). Its diacylglycerol backbone carries a phosphate esterified to choline. Therefore, we used [^{3}H]-choline for studying lipid metabolism during HSV-1 infection. For this, we added 1 μCi/ml [^{3}H]-choline 4 h prior to harvesting, isolated nuclei, and extracted lipids from both the nuclear and cytoplasmic fraction. Scintillation counting revealed a significant higher level of [^{3}H]-choline in the nuclear fraction at 9, 12 and 16 hpi (Fig. 2A), and in the cytoplasmic fraction at 12 and 16 hpi (Fig. 2B) of HSV infected cells compared to mock infected cells. Therefore, we concluded that *de novo* synthesized phospholipids are incorporated first into nuclear membranes and later also into cytoplasmic membranes during HSV-1 infection. Since virions can be transported into RER cisternae some of the radioactivity may be related to the viral envelope of these virions that originated from budding at the INM.

[^{3}H]-choline is incorporated into viral envelopes

Formation of progeny virus requires large amount of membranes that may derive from budding at INM, ONM, RER (Darlington and Moss, 1968; Leuzinger et al., 2005), and at Golgi membranes. To assess whether *de novo* synthesized lipids are used for viral envelopment we exposed HSV-1 infected cells to [^{3}H]-choline for 4 h at 10 hpi and harvested virus at 24 hpi. Inspection by TEM revealed that the purification did not result in entirely pure virus fractions. Nonetheless, the statistically significant difference in the amount of [^{3}H]-choline between HSV-1 samples and mock samples is assumed to be due to the presence of virions. Therefore, the signal of [^{3}H]-choline measured in lipids extracted from the intracellular virus fraction and extracellular virus fraction (Fig. 2) indicates that *de novo* synthesized phospholipids became part of the viral envelope. Addition of BFA 15 min prior to [^{3}H]-choline exposure resulted in a decline of radioactivity of about ~40% compared to untreated cells. The number of intracellular virions, compared to virions harvested from untreated cells, was ~60% lower (Fig. 2C). BFA disassembles the Golgi complex within minutes (Hess et al., 2000) which led to accumulation of virions in the PNS and RER cisternae (Fig. 3). Therefore, we conclude that [^{3}H]-choline incorporated into nuclear membranes became part of the viral envelope during budding of capsids at the INM and that [^{3}H]-choline remained in the envelope of virions which were transported from the PNS into RER cisternae. Radioactivity in samples supposed to contain extracellular virions was low after BFA treatment but significantly higher

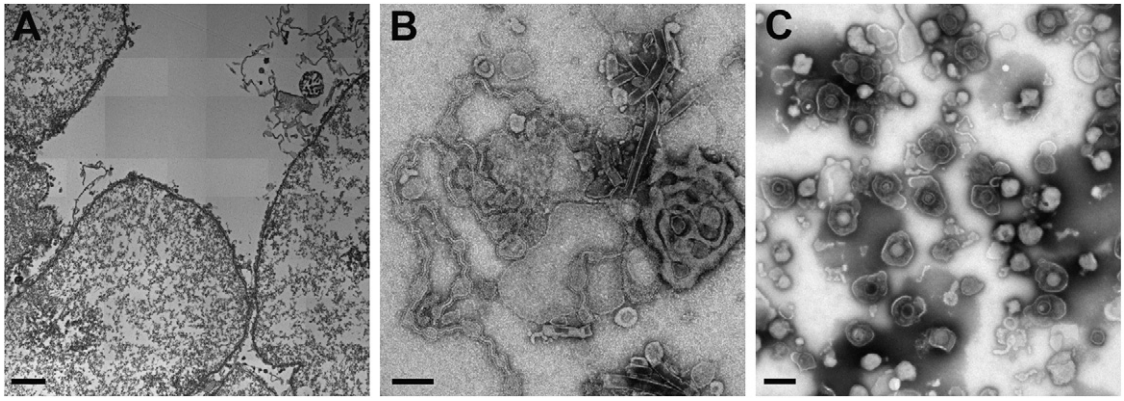

Fig. 1. Electron micrograph of (A) the nuclear fraction showing nuclei surrounded by intact INM but disrupted ONM and some additional cytoplasmic membranes, (B) cytoplasmic fraction containing pure membranes, and (C) isolated virions contaminated with some membranous fragments which may have derived from cellular membranes but also from viral envelopes.

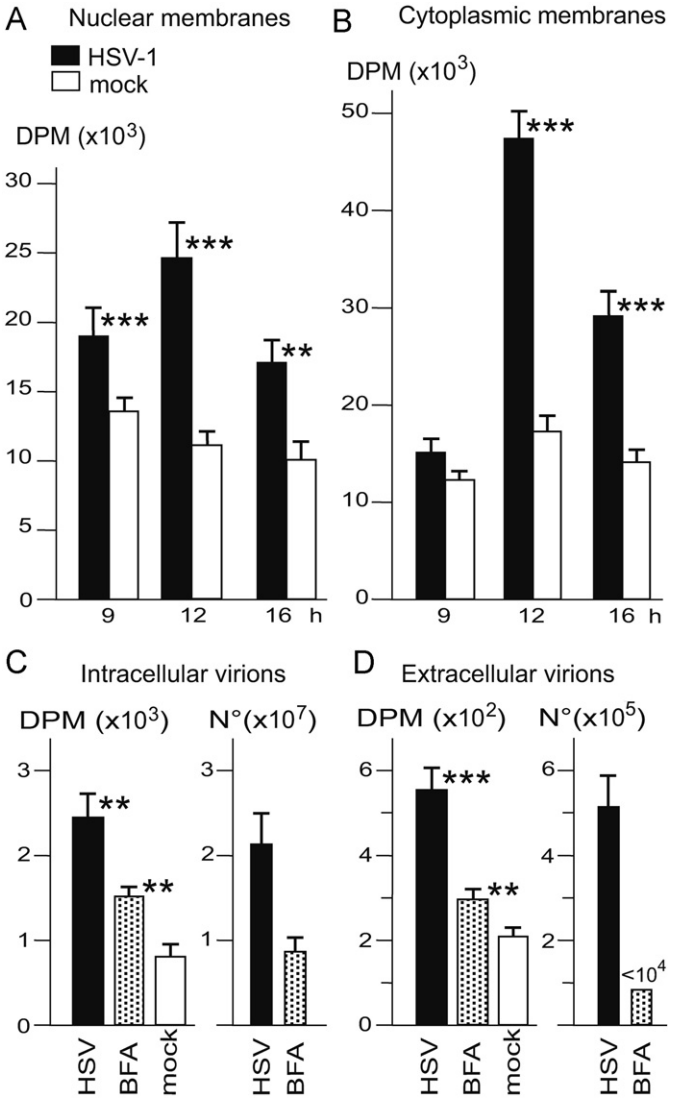

Fig. 2. [^{3}H]-choline incorporation into nuclear lipids (A) and cytoplasmic lipids (B) in cells exposed to 1 μCi/ml [^{3}H]-choline 4 h prior to harvesting for lipid extraction was significantly higher after HSV-1 infection than after mock infection. [^{3}H]-choline incorporation into the viral envelope of intracellular (C) and extracellular virions (D) after exposure to BFA from 10 to 14 hpi in cells harvested at 24 h after inoculation with HSV-1 at MOI 5. Despite purification did not result in absolute pure virus fractions the statistical difference between HSV-1 samples and mock samples is assumed to account for the presence of lipids from the viral envelope. The approximate number of virions were determined by TEM on negatively stained samples and calculated per 300 μl volume obtained after purification. Level of significance $^{**}p < 0.01$, $^{**}p < 0.001$, $n=4$.

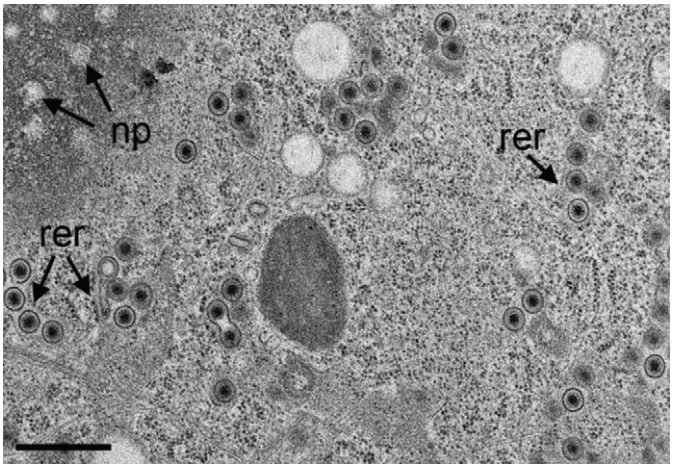

Fig. 3. TEM image taken from a HSV-1 infected cell exposed to BFA at 8 hpi and harvested at 24 hpi as described in material and methods. The RER (rer) is congested with virions. The nucleus is tangentially sectioned so that nuclear pores (np) become apparent. Bar, 500 nm.

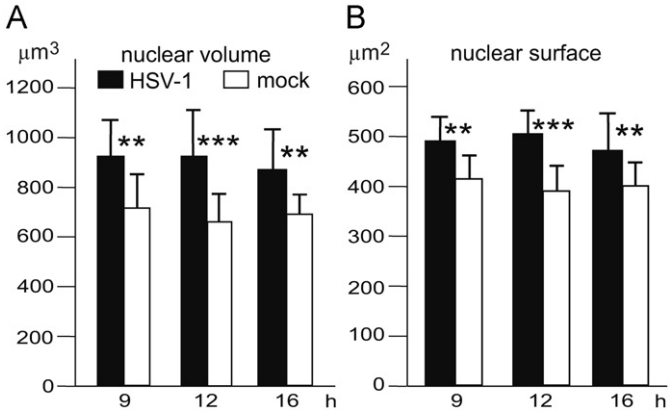

Fig. 4. Nuclear volume (A) and nuclear surface area (B) of HSV-1 or mock infected cells as calculated from confocal microscopic images. Mean nuclear volume of HSV-1 infected cells was by a factor of 1.3–1.5 significantly larger compared to mock infected cells, and the nuclear surface by a factor of 1.16–1.28 at 9, 12 and 16 hpi. Level of significance $^{**}p < 0.01$, $^{***}p < 0.001$, $n=25$.

than in samples obtained from mock infected cells (Fig. 2D). The detection limit of the method applied is 10^4 particles/10 μl (Laue et al., 2009). Though the radioactivity in samples, which are supposed to contain extracellular virions, was significantly higher than in samples obtained from mock infected cells (Fig. 2D) it cannot be deduced with certainty that the higher radioactivity was due to [^{3}H]-choline of extracellular virions.

Nuclear volume increases during HSV-1 infection

Nuclear volume has been shown to increase in HEp-2 cells (Simpson-Holley et al., 2005), H2B cells (Monier et al., 2000) and Vero cells (Wild et al., 2009) infected with HSV-1. To quantify alterations at the membrane compartments concerned with envelope formation we first determined the nuclear volume and the nuclear surface area on confocal images on the basis of the half axes a, b and c. Nuclear volume of HSV-1 infected Vero cells was by a factor of 1.27 higher at 9 hpi compared to mock infected cells (Fig. 4A). The nuclear surface area was 1.15 times higher than in mock infected cells (Fig. 4B). Theoretically, the surface is expected to enlarge by a factor of 1.15 if the volume expands by a factor of 1.27 indicating that the calculation of the surface are based on the measured axes is fairly appropriate. After 9 hpi, nuclei did not further expand. Expansion of nuclear volume and surface area demands enlargement of nuclear membranes suggesting that the incorporated [^{3}H]-choline was used for *de novo* phospholipid synthesis to maintain membrane integrity early in infection. After 9 hpi, however, nuclear size remained constant. Therefore, [^{3}H]-choline incorporation later in infection is considered very likely to be needed for viral envelopment by budding of capsids at the INM. To investigate the fate of these membranes, we next carefully examined the nuclear periphery in cells prepared for electron microscopy at improved resolution.

Neither inner nor outer nuclear membrane enlarges in addition to nuclear expansion

If it was true that perinuclear virions are de-enveloped by fusion with the ONM the ONM would be expected to enlarge – at

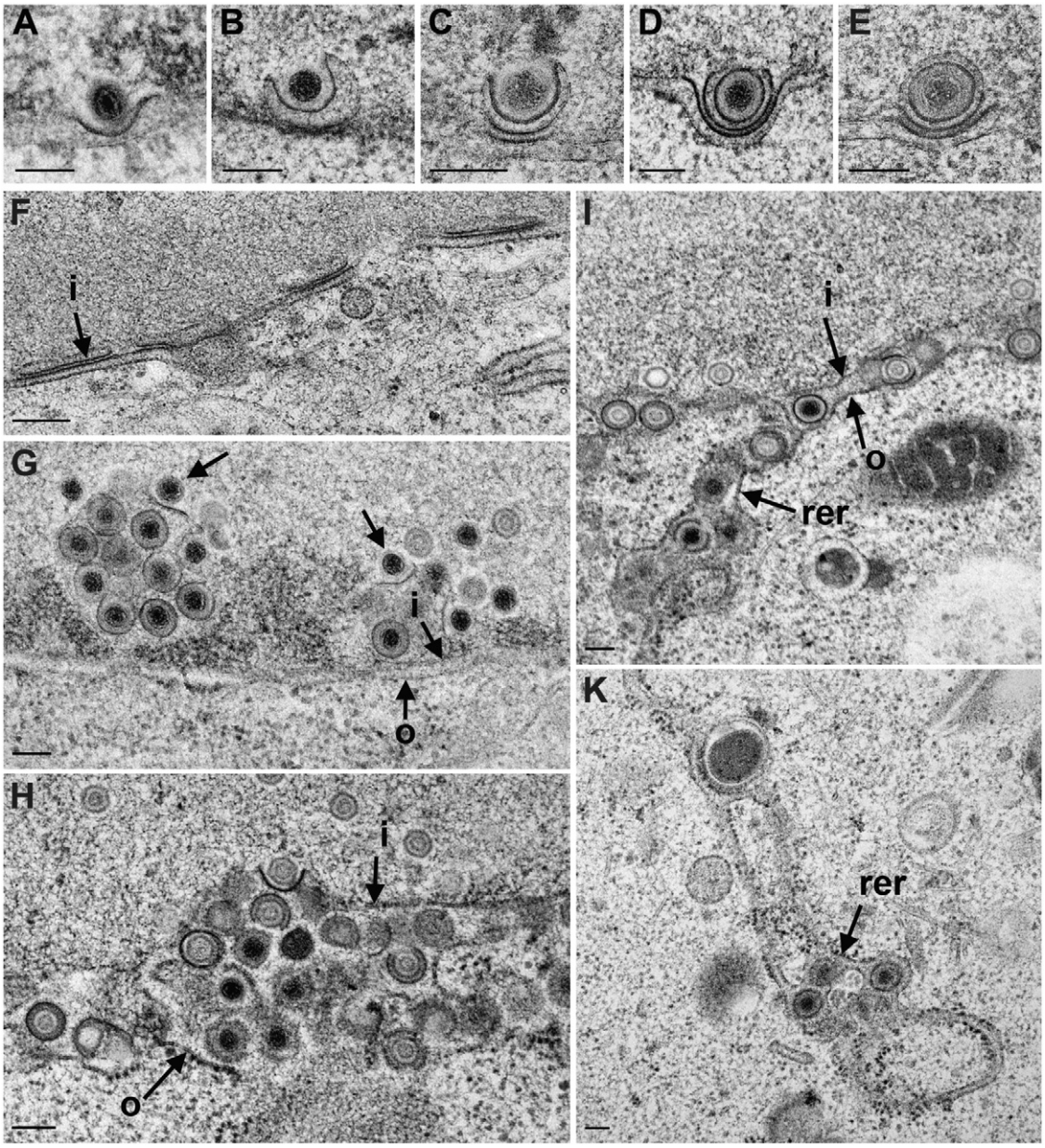

Fig. 5. The nuclear periphery of HSV-1 infected cells at 16 hpi or 20 hpi (H) imaged by TEM of cryo-fixed monolayers. (A) Budding of capsids starts by thickening of the INM that becomes the viral envelope. (B–E) Later in infection budding may be accompanied by duplication of the INM finally resulting in formation of a vacuole or a pouch. (F) Duplication of the INM (i) seems to occur independently from budding. (G) Accumulation of virions between the ONM (o) and INM (i) with a budding capsid. (H) Virions in the PNS and RER at 20 hpi. (I) The PNS continues into the RER; both contain virions. (K) RER at the cell periphery containing virions. Bars, 200 nm.

least temporarily – possibly forming folds and/or duplications. Transmission electron microscopy revealed that the INM and ONM are layered in parallel at 9 and 12 hpi. However, at 16 hpi, the INM was found to form duplication mainly at sites of budding capsids (Fig. 5A to F) as well as invaginations at which capsids bud (Fig. 5G). The ONM did not show any folds or duplications. Morphometric analysis performed on 25 nuclei selected at random did not reveal any statistical difference of the surface area between INM and ONM (data not shown) indicating that nuclear membranes did not enlarge in addition to the overall enlargement related to nuclear expansion as shown by confocal microscopic analysis. On the other hand, virions accumulated in the PNS (Fig. 5G and H) and in adjacent RER cisternae (Fig. 5I) suggesting that a considerable amount of membranes are used for envelopment, and that these membranes are not immediately inserted into the ONM via fusion. Consequently, large amounts of membrane constituents must be provided for budding at the INM. Furthermore, virions were found in RER cisternae elsewhere in the cytoplasm (Fig. 5K) leading to the assumption of intraluminal transportation form the PNS into the RER.

Numerous capsids bud simultaneously trough the nuclear membrane

For transmission electron microscopy, sections of 50–80 nm thickness are prepared. The chance to find a budding capsid in a given section plane through the nucleus is thus rather low. The highest mean number of budding capsids was 1.25 per nuclear profile at 12 hpi counted on 25 randomly selected cell profiles. Therefore, we applied a sophisticated cryo-technique for visualization of the nuclear surface in the frozen hydrated state by scanning electron microscopy. As shown in Fig. 6, more than

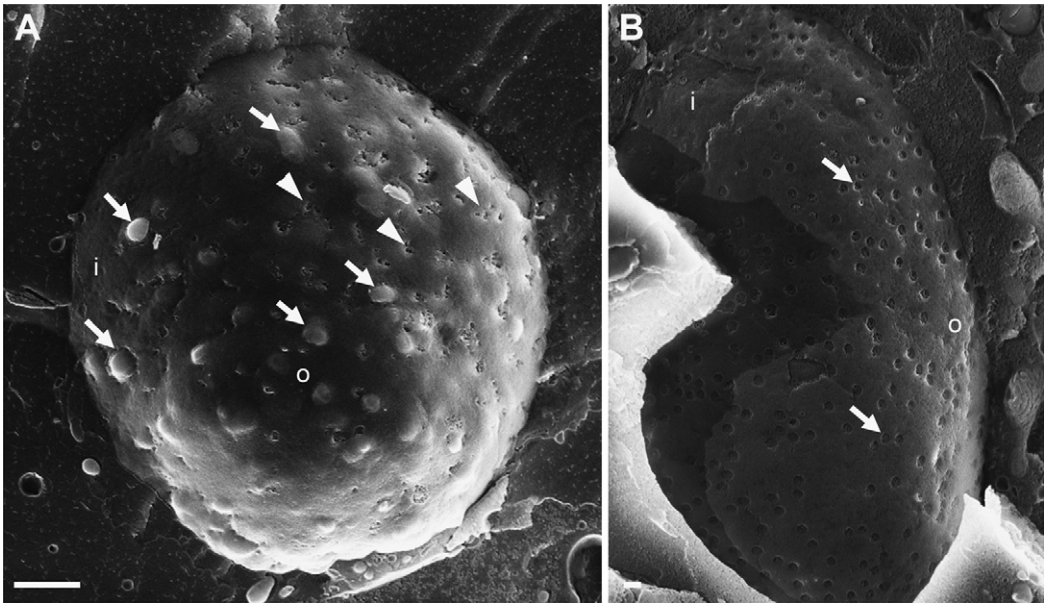

Fig. 6. (A) View onto the ONM (o) and a small area of the INM (i) in a HSV-1 infected cell 14 hpi imaged by Cryo-FESEM exhibiting at least 25 budding capsids (some are indicated by arrows) and irregularly distributed nuclear pores (arrowheads) and (B) nuclear surface of a mock infected cell with hundreds of nuclear pores. Bars, 400 nm.

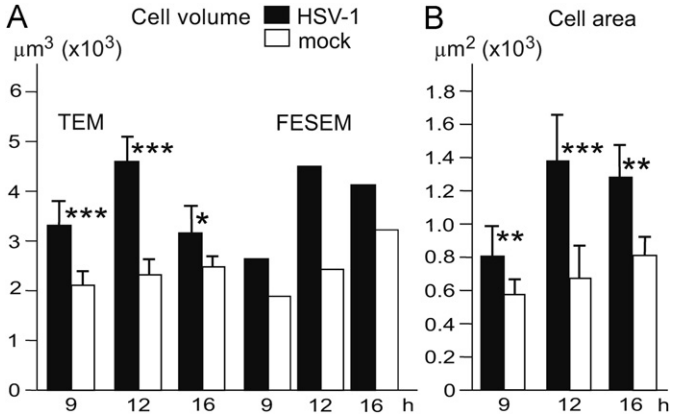

Fig. 7. (A) Cell volume of HSV-1 or mock infected cells calculated on the basis of the nuclear volume and data obtained by morphometry on TEM images as described in material and methods, and (B) of hypothetical cone-shaped cells calculated on the basis of the cell area measured on FESEM images shown in Fig. 7. Level of significance $^{*}p<0.05$, $^{**}p<0.01$, $^{***}p<0.001$, $n=25$.

25 capsids bud simultaneously at the nuclear surface. The diameter of enveloped virions is about 200 nm, the surface area of the viral envelope 0.125 μm^2. Therefore, a minimum of 3.1 μm^2 membrane area, equaling ~500,000 phospholipid molecules (Kucerka et al., 2006), needs to be supplied instantly.

Cell volume increases after HSV-1 infection

The mean cell volume was calculated on the basis of the nuclear and cytoplasmic density obtained by morphometric analysis of electron micrographs at low magnification, and on the nuclear volume obtained from confocal images. The mean cell volume of HSV-1 infected cells was ~3400 μm^3 at 9 and 16 hpi, and about ~4800 μm^3 at 12 hpi compared to ~2000 μm^3 (9 and 12 hpi) and ~2300 μm^3 (16 hpi) of mock infected cells (Fig. 7A). These data are fairly in line with the volume of the hypothetical cone-shaped cells calculated on the basis of the cell area (Fig. 7B) measured in FESEM images (Fig. 8) so that the cell volume is probably not, or not much, overestimated. Even though the data were overestimated e.g. at 12 hpi the conclusion can be drawn that cell volume increases during the first 12 h of HSV-1 infection. The cell surface area also enlarges concomitantly to cell volume expansion as can be roughly estimated on FESEM images (Fig. 8). Hence phospholipids are required for maintaining plasma membrane integrity during cell expansion starting early in infection.

The RER is temporarily enlarged during HSV-1 infection

The ONM continues into RER lamellae so that virions can be transported from the PNS into RER cisternae (Fig. 5I and K). Membranes inserted into the ONM during de-envelopment may hence be shifted to adjacent RER lamellae that would result in enlargement of the RER. Therefore, we estimated the surface density of the RER (Sv_r) by morphometric analysis applying the point counting method (Weibel, 1979), and calculated its surface area (S_r) per mean cell volume (Fig. 9A). The surface area of the RER (S_r) was significantly enlarged at 12 hpi compared to 9 hpi ($p<0.001$), and to mock infected cells ($p<0.001$). At 16 hpi, however, S_r was again at the level at 9 hpi. The number of capsids in the cytoplasmic matrix was lower at 12 hpi compared to 16 hpi (Fig. 9B). This suggests that the membranes responsible for RER enlargement are not viral envelopes of perinuclear virions that fused with RER membranes or with the ONM followed by subsequent shifting to the RER. RER expansion might be rather related to enhanced lipid synthesis (van Meer et al., 2008) and/or to the synthesis of vast amounts of proteins necessary for herpes virus replication.

The Golgi complex enlarges prior to fragmentation

The Golgi complex is a highly dynamic organelle that may enlarge by 150% within 12 h after a short initial stimulation for secretion of parathyroid hormone (Wild et al., 1985). The Golgi complex is difficult to study because of its shape and its sensitivity to improper fixation and processing for electron microscopy (Wild et al., 2001). Electron microscopy based on cryo-fixation, which leads to improved retention of lipids (Weibull et al., 1984) and improved spatial and temporal resolution, revealed intact Golgi fields consisting of varying numbers of stacks in mock and HSV-1 infected cells. To quantify changes in the size of the Golgi complex during HSV-1 infection we

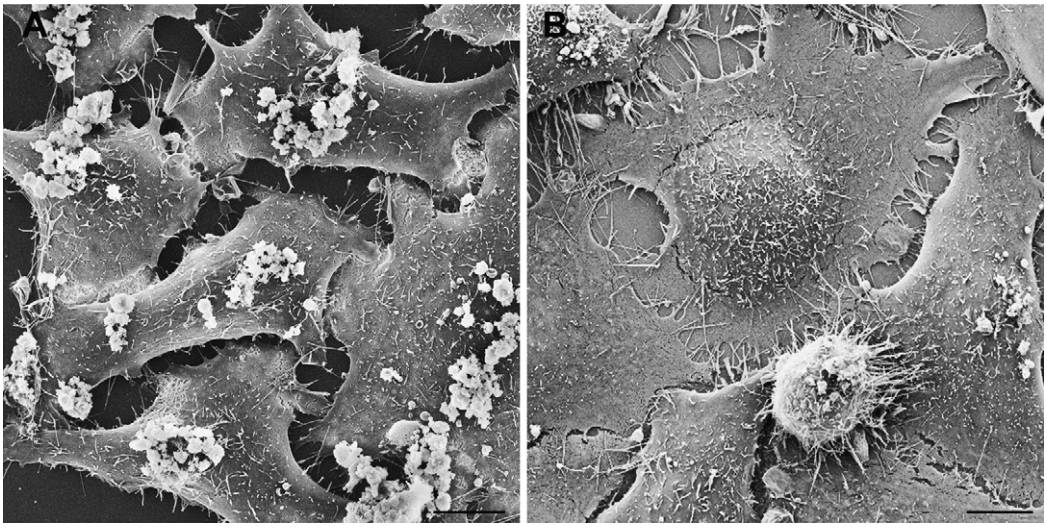

Fig. 8. FESEM images of mock (A) and HSV-1 and (B) infected cells at 12 hpi demonstrating enlargement of cells in HSV-1 infection. Bars, 10 μm.

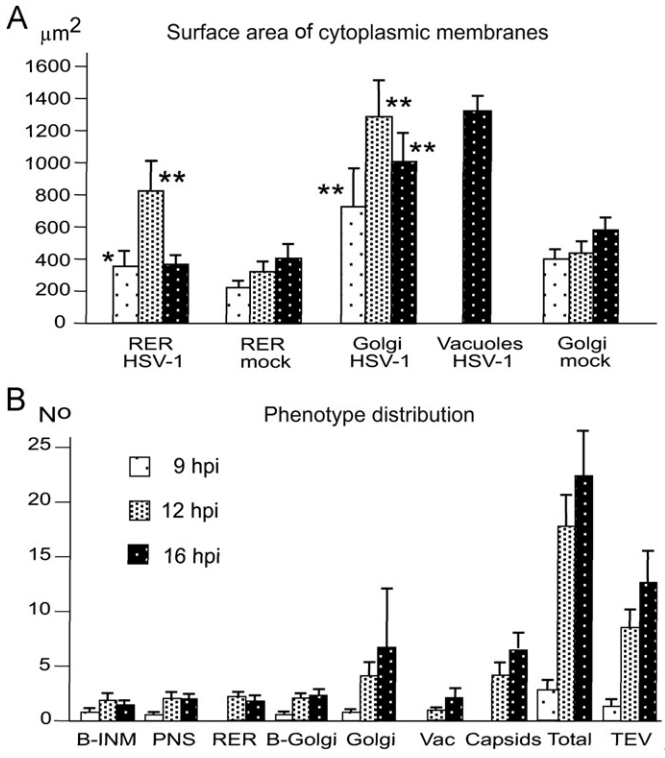

Fig. 9. (A) Surface area of RER, Golgi complex and vacuoles containing virions was estimated by morphometric analysis of 5 independent experiments. RER was significantly larger at 9 and 12 hpi after HSV-1 infection than after mock infection whereas the Golgi complex was larger at any time point of sampling. Considering that membranes of vacuoles originated from the Golgi complex the entire surface at 16 hpi is more than twice of the size at 12 hpi. Level of significance $^{*}p<0.01$, $^{**}p<0.001$, $n=5$ and (B). Phenotype distribution in HSV-1 infected cells at 9, 12 and 16 hpi. B-INM=budding capsids at the INM, B-Golgi=budding capsids at Golgi membranes, Vac=virions in transport vacuoles, Capsids=naked capsids in the cytoplasm, Total=total of virus particles, TEV=total enveloped virus particles.

estimated its surface density (Sv_g) by morphometric analysis, and calculated the absolute surface area of the Golgi complex (S_g) per mean cell volume. The data (Fig. 9A) show significant enlargements of Golgi membranes at 9, 12 and 16 hpi compared to mock infected cells. The surface area (S_g) at 9 hpi was 112% larger compared to that of mock infected cells. At 12 hpi it was 71% larger than at 9 hpi, and 278% higher compared to mock infected cells. At 16 hpi, the S_g of intact Golgi cisternae was reduced but still 15% higher than at 9 hpi and 58% larger compared to mock infected cells. Adding the surface area of transport vacuoles to that of Golgi membranes at 16 hpi, the total surface area was 305% larger compared to the Golgi complex at 9 hpi. The data suggest that enhanced synthesis of membrane constituents has started prior to 9 hpi to provide membranes for the Golgi complex that is needed for envelopment and formation of transport vacuoles. Budding of capsids at Golgi membranes, a process referred to as wrapping, results in concomitant formation of a concentric vacuole containing a single virion (Leuzinger et al., 2005). The mean number of capsids involved in envelopment by wrapping was ~1/cell profile at 12 hpi and ~2/cell profile at 16 hpi (Fig. 9B). On the other hand, Golgi fields contained fully enveloped virions within cisternae. The mean number of virions in Golgi cisternae was ~4/cell profile and ~7/cell profile at 12 and 16 hpi, respectively. Golgi membranes exhibited indications for fission (Fig. 10A). Fission is assumed to result in transport vacuoles as a normal event in the secretory pathway (Palade, 1975). Vacuoles or dilated Golgi cisternae showed up to 10 virions in a given section plane (Fig. 10B and C) raising the questions how and where the particles had entered the vacuoles. After 16 hpi, the Golgi complex did not appear as an entity (Fig. 10D). Enlargement of the surface area of Golgi membranes and the high number of virions suggest that *de novo* synthesized phospholipids are needed to facilitate viral envelopment at the Golgi level and formation of transport vacuoles.

HSV-1 reduces fluid-phase endocytosis

Constituents inserted into the plasma membrane during exocytosis are known to recycle back to the Golgi complex in secretory cells (Orci et al., 1981). To investigate whether enlargement of the Golgi complex could be due to incorporation of recycled plasma membrane constituents fluid-phase endocytic activity was assayed by measuring the uptake of HRP. Medium was replaced by medium containing HRP after 5, 9, 12 and 16 hpi, and HRP uptake was measured 15 min after incubation. Endocytotic activity in HSV-1 infected cells remained unchanged between 5 and 16 hpi whereas it significantly increased in mock infected cells (Fig. 11), indicating that fluid-phase endocytosis at least is not involved in enlargement of the Golgi complex.

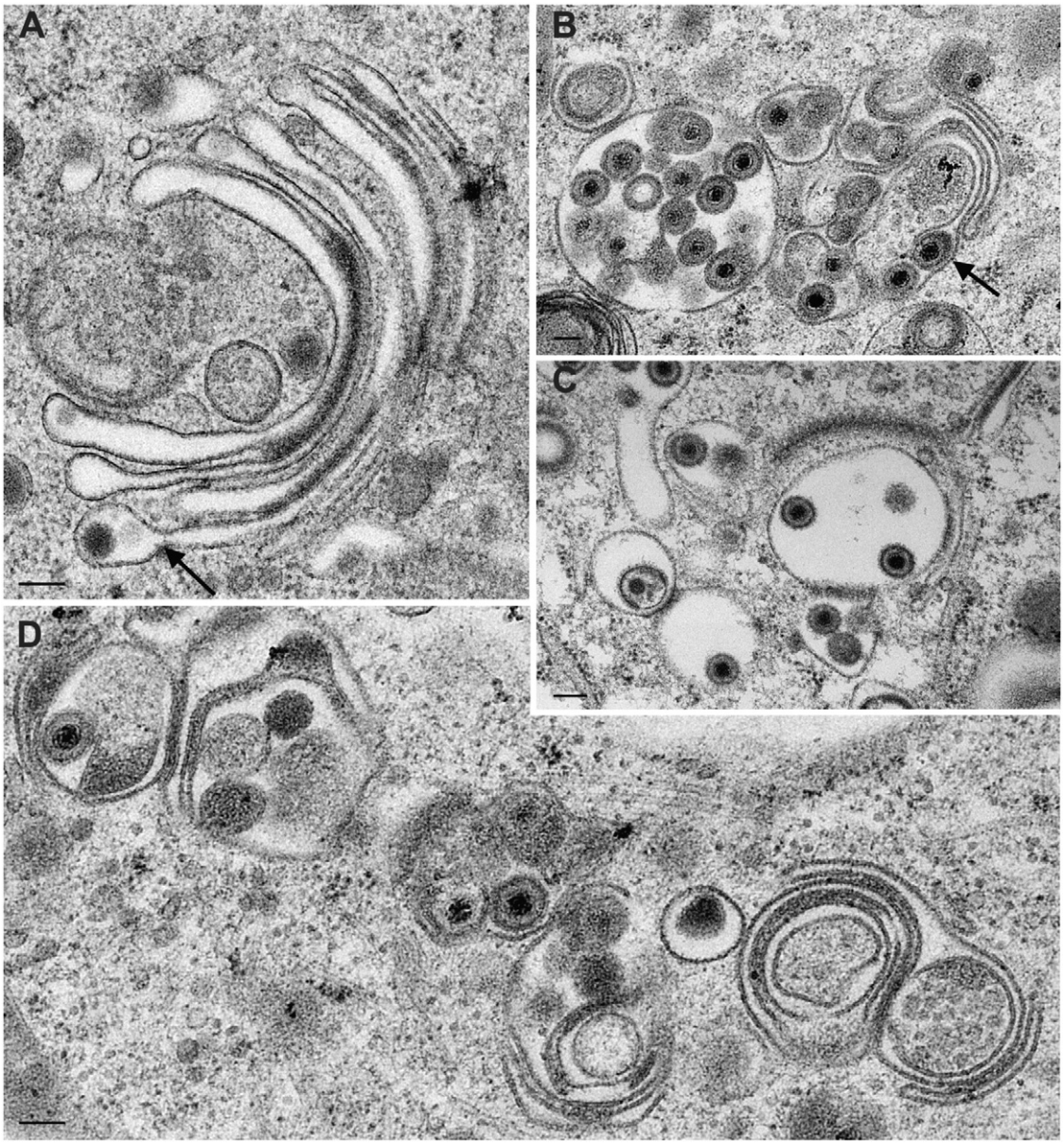

Fig. 10. TEM images of the Golgi complex and vacuoles in HSV-1 infected Vero cells. (A) Golgi complex at 12 h of HSV-1 infection containing a tangentially sectioned virion in a laterally dilated cisterna with indications for fission (arrow). Note focal thickening of membranes by deposition of an electron dense substance. (B–D) At 16 hpi Golgi membranes are dispersed over large areas. Golgi cisternae (arrow) and vacuoles contain one or numerous, often tangentially sectioned virions. Whether these structures are true vacuoles or whether they are dilated Golgi cisternae cannot always be addressed in a given section plane. Bars, 200 nm.

HSV-1 inhibits mitosis

Phospholipid metabolism in growing cells depends to a large extend on the cell cycle. Signals promoting phospholipid synthesis act early in G1 or even in M phase (Jackowski, 1996). However, arrested cells continue to produce phospholipids (Jackowski, 1994; Jackowski, 1996). HSV-1 arrests the cell cycle in the G1/S phase and S phase (de Bruyn Kops and Knipe, 1988; Ehmann et al., 2000) that may lead to reduction of phospholipid synthesis related to mitotic activity. Determination of the mitotic rate revealed that cell cycle is blocked by HSV-1 leading to nearly complete decline of mitotic activity at 6 hpi whereas mitotic activity in mock infected cells declined much later (Fig. 12). The significantly higher incorporation of [^{3}H]-choline into phospholipids of cell cycle arrested cells suggest that HSV-1 stimulates per se phospholipid synthesis.

Discussion

Budding of capsids at the INM requires membranes that need to be supplied either prior to or concomitantly to budding. If capsids are released from the PNS into the cytoplasm via de-envelopment the viral envelope has to fuse with the ONM. Consequently, the ONM will enlarge by the amount of the inserted membrane area corresponding to the surface area of the number of viral envelopes that fuses with the ONM. Therefore, the ONM gets folded as a result of this membrane insertion unless the equivalent of the inserted membrane area is shifted to the RER, which would lead to RER expansion, or recycled to the INM, e.g. by lateral movement at sites of nuclear pores (Fig. 13). If membrane constituents will recycle back to the INM they can be reused for budding. In this case, no or little additional phospholipids are needed to enable budding at the INM. An alternative

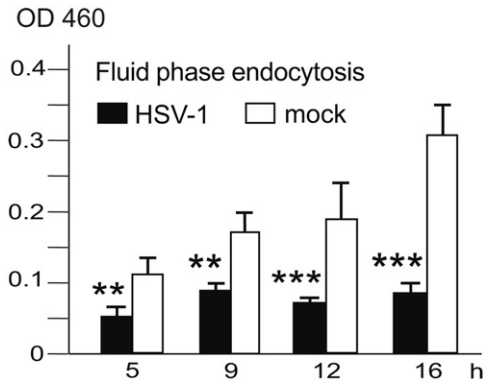

Fig. 11. Fluid phase endocytosis of HRP by Vero cells infected with HSV-1 compared to mock infected cells. HRP uptake remained constant in HSV-1 infected cells but was significantly increased in mock infected cells at 9, 12 and 16 h of incubation. Level of significance $^{**}p < 0.01$, $^{***}p < 0.001$, $n=3$.

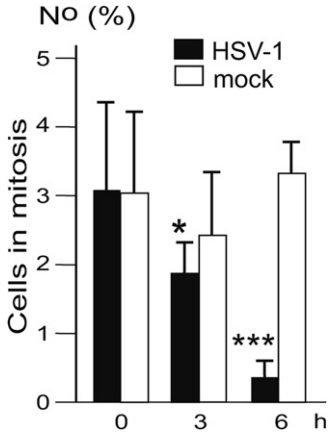

Fig. 12. Percentage of cells in mitosis determined by counting DAPI stained nuclei. The rate of cells in mitosis declined to 1.8% at 3 hpi, and was close to zero at 6 hpi with HSV-1 compared to mock infected cells. Level of significance $^{*}p < 0.05$, $^{***}p < 0.001$, $n=6$.

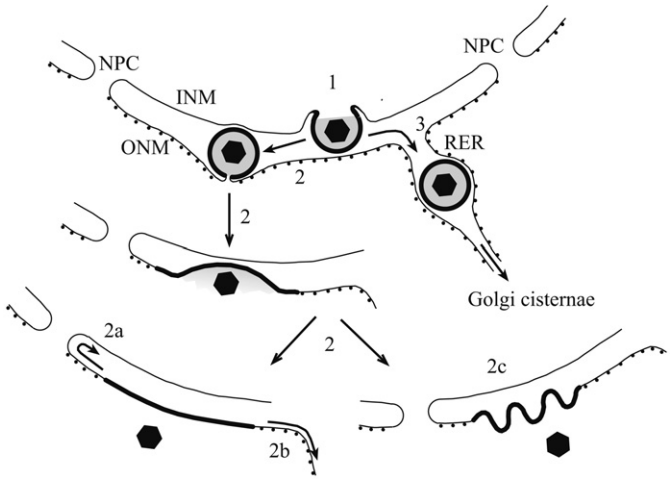

Fig. 13. Possible fate of the viral envelope derived by budding at the INM. 1) Budding of capsids results in loss of INM that needs to be replaced. 2) Insertion of INM into the ONM by fusion resulting in enlargement of the ONM. 2a) Inserted INM might be shifted back along the rim of nuclear pores. 2b) Inserted membranes might be shifted into RER membranes. 2c) Enlarged ONM might become folded. 3) INM remains on the viral envelope during intraluminal transportation into Golgi cisternae for packaging. Note: fusion starts immediately after close apposition of two membranes followed by formation of the fusion pore. The characteristic feature of virions in the PNS is the dense envelope. After fusion with the ONM the inserted dense membrane equals the surface of the viral envelope.

pathway for virions to be released from the PNS is by intraluminal transportation via adjacent RER cisternae directly into the Golgi complex for packaging into transport vacuoles. In this case, large amounts of membranes are needed for capsid envelopment at the nuclear level.

Incorporation of [^{3}H]-choline detected in the nuclear fraction clearly indicates that phospholipids are supplied by *de novo* synthesis induced by HSV-1. Newly synthesized phospholipids are probably required early in infection for maintaining membrane integrity of nuclei that expand during HSV-1 infection as also shown for HEp-2 (Simpson-Holley, 2005) as well as for maintaining plasma membrane integrity of expanding cells. Later in infection, it is considered very likely that *de novo* synthesized phospholipids are predominantly required for capsid envelopment because of the following reasons: i) on average, 1.83 capsids/μm^2 bud at the INM 12 hpi with HSV-1 (Wild et al., 2009) giving a total of ~915 capsids per mean nuclear surface of 500 μm^2. The surface area of the envelope of a HSV-1 virion with a diameter of 200 nm (Grunewald et al., 2003) is 0.125 μm^2, consequently that of 915 capsids 115 μm^2. This is 23% of the entire nuclear surface at 12 hpi. ii) HSV-1 virions accumulate in the PNS (Fig. 5) as repeatedly shown in HSV-1 infected cells (Campadelli-Fiume et al., 1991; Darlington and Moss, 1968; Stannard et al., 1996; Torrisi et al., 1992). Virion accumulation in the PNS is enhanced late in infection (Leuzinger et al., 2005) or after BFA treatment (Whealy et al., 1991). In cells infected with HSV-1 mutants lacking glycoprotein B (Farnsworth et al., 2007) or US3 (Poon et al., 2006; Reynolds et al., 2002; Wisner et al., 2009) huge numbers of virions accumulate in the PNS. All these virions originated by budding through the INM. iii) HSV-1 virions have access to RER cisternae (Fig. 5) as has been shown by many authors (Farnsworth et al., 2007; Gilbert et al., 1994; Granzow et al., 1997; Nii et al., 1968; Radsak et al., 1996; Schwartz and Roizman, 1969; Stannard et al., 1996). The presence of virions within RER cisternae indicates intraluminal virion transportation from the PNS into adjacent RER cisternae (Nii et al., 1968; Schwartz and Roizman, 1969). If these virions are indeed intraluminally transported, the envelope originated from the INM is not inserted into the ONM. iv) [^{3}H]-choline was detected in intracellular virions after BFA treatment which results in Golgi disassembly within minutes (Hess et al., 2000) and in accumulation of virions in the PNS and RER. Fig. 3 shows at least 32 virions within RER cisternae proving that virions can be intraluminally transported and that their envelopes are definitely not inserted into the ONM.

De-envelopment by fusion of all the viral envelopes with the ONM would result in substantial enlargement of the ONM as outlined above. Besides a few duplications, there were no indications for nuclear membrane enlargement besides that related to nuclear expansion. The ONM is part of the RER. Membrane constituents may be shifted towards the RER. The RER was only temporarily enlarged early in infection suggesting that it was not related to budding of capsid at the INM followed by de-envelopment. RER enlargement rather reflects enhanced synthesis of phosphatidylcholine (van Meer et al., 2008). If de-envelopment really takes place membrane constituents may recycle back to the INM and can be reused for envelopment. In this case, no newly synthesized phospholipids are required. [^{3}H]-choline incorporation peaking at 12 hpi does not support this idea.

Virions located in the PNS have the ability for intraluminal transportation into RER, which was demonstrated to continue into Golgi complex (Leuzinger et al., 2005; Wild et al., 2002). These virions can then be transported directly into Golgi cisternae for packaging into transport vacuoles following the well known secretory pathway (Palade, 1975). In this case, the INM would be the final envelope of some of the progeny virus implying that phospholipid composition of the viral envelope would be identical to that of the INM. Lipid analyses of the HSV-1 envelope revealed

that its phospholipid composition was more similar – but by no means identical – to the phospholipid composition of Golgi membranes than to that of nuclear membranes (van Genderen et al., 1995). This led to the suggestion that phospholipid composition of cell membranes involved in envelope formation might alter during infection (van Genderen et al., 1995). If the viral envelope indeed derives from both nuclear and Golgi membranes as suggested (Leuzinger et al., 2005) its lipid composition will be a combination of the phospholipids of these two membrane compartments. Interestingly, phospholipids composition of pseudo rabies virus envelope was shown to resemble more that of the inner nuclear membrane (Ben-Porat and Kaplan, 1971).

[^{3}H]-choline was also incorporated into membranes of the cytoplasmic fraction. It can be deduced from the morphometric data that newly synthesized phospholipids were used for enlargement of the RER early in infection, to maintain plasma membrane integrity during cell expansion, and to provide membranes for envelopment at the Golgi level. Capsids bud at the trans Golgi network (Mettenleiter, 2004; Mettenleiter et al., 2006) or into Golgi cisternae or Golgi derived vacuoles (Homman-Loudiyi et al., 2003; Leuzinger et al., 2005). After BFA treatment, envelopment at the Golgi level ceases. The radioactivity detected on isolated intracellular virions after BFA treatment was ~40% lower than that detected on virions isolated from untreated cells. This suggests that in untreated cells ~60% of the signals may have derived from viral envelopes acquired by budding at nuclear membranes, and ~40% by budding at Golgi membranes. The radioactivity detected in samples supposed to contain extracellular virions is assumed to be related to virions released after cell lysis.

Our data indicate that newly synthesized phospholipids are used for envelopment at both the nuclear and Golgi level, which is in line with data obtained from [^{3}H]-choline labeling of pseudo rabies virus infected rabbit kidney cells (Ben-Porat and Kaplan, 1971; Ben-Porat and Kaplan, 1972). Choline is esterified to diacylglycerol forming phosphatidylcholine, and to ceramide forming sphingomyelin. Phosphatidylcholine is the most abundant phospholipid in eukaryotic cell membranes comprising 40–50% of the phospholipid mass. It contributes ~58% of the phospholipids in nuclear and RER membranes, and ~55% to Golgi membranes (Henneberry et al., 2002). Sphingomyelin is present on Golgi membranes contributing ~15% of the phospholipids (van Meer et al., 2008). Therefore, [^{3}H]-choline is an excellent compound for studying phospholipid metabolism. In contrast to [^{3}H]-choline, incorporation of [^{32}P]-phosphate, [^{3}H]-ethanolamine and [^{14}C]-ethanolamine was unaltered or even decreased in HSV-2 infected cells (Daniel et al., 1981).

In conclusion, this study, combining for the first time labeling of phospholipid precursors and morphometric analysis of organelles involved in envelopment, revealed clear evidence that HSV-1 induces *de novo* synthesis of phospholipids, which are required for maintenance of membrane integrity of expanding nuclei early in infection, for formation of viral envelops by budding at the INM and at Golgi membranes, and for formation of vacuoles for transportation of virions towards the cell periphery. The data favor the theory of intraluminal virion transportation out of the PNS resulting in loss of nuclear membranes produced on a large scale to enable budding of capsids at the INM.

Materials and methods

Cells and viruses

Vero cells (European Collection of Cell Cultures) were grown in Dulbecco's modified minimal essential medium (DMEM; Gibco, Bethesda, MD) supplemented with penicillin (100 U/ml), streptomycin (100 μg/ml) and 10% fetal calf serum (FCS; Gibco). Wild-type HSV-1 strain F was propagated in Vero cells.

Infection of cells

Cells were infected with HSV-1 at a multiplicity of infection (MOI) of 5 plaque forming units (PFU) per cell in DMEM without FCS and kept at 37 °C for 1 h to allow adsorption prior to incubation at 37 °C in DMEM supplemented with 2% FCS or without FCS.

[^{33}H]-choline incorporation

Cells were grown in 75 cm^2 tissue culture flasks for 48 h prior to inoculation with HSV-1 in low choline content (1 mg/l) Eagle's minimal essential medium (EMEM; Bioconcept, Allschwil, Switzerland). For assessment of [^{3}H]-choline incorporation into cytoplasmic and nuclear membranes, medium was replaced by 4 ml medium containing 1 μCi/ml [^{3}H]-choline (PerkinElmers, Waltham, MA, USA) 4 h prior to harvesting. Cells were harvested using trypsin at 9, 12 or 16 hpi for lipid extraction from both the nuclear and cytoplasmic fraction to determine [^{3}H]-choline concentration by scintillation counting. 25 μl aliquots were removed to determine the actual cell number for normalization of counts.

For measurement of [^{3}H]-choline incorporation into viral envelopes, cells were grown in 75 cm^2 tissue culture flasks for 48 h prior to inoculation with HSV-1 (MOI 5) in low choline content medium. Cells were exposed to 1 μCi/ml [^{3}H]-choline (4 ml medium) from 10 to 14 hpi. Brefeldin A (BFA, 1 μg/ml medium) was added to the medium 15 min prior to [^{3}H]-choline exposure. At 24 hpi, extracellular virus was harvested from the medium, and cell associated virus was isolated after two sequences of freezing (−80 °C) and thawing of the cell cultures. Virus was purified by centrifugation through 25% sucrose in Hanks balanced salt solution (HBSS; Gibco) at 52,000 g for 2 h at 4 °C. Pellets were re-suspended in 300 μl H_2O. Lipids were extracted as described below.

For determination of the actual number, virions were adsorbed for 10 min onto carbon coated parlodion films mounted on 300 mesh/inch copper grids by placing them on 10 μl droplets of viral suspension, briefly washed and stained with Na-phosphotungstic acid, pH 7.0, for 1 min as described (Wild, 2008). Virions were counted on 5 different fields under a TEM (CM12; Philips, Eindhoven, The Netherlands) and calculated per 300 μl viral suspension.

Separation of nuclear and cytoplasmic fraction

Cells grown in 75 cm^2 tissue culture flasks were detached using trypsin and collected in 10 ml medium. Nuclei were isolated in ice-cold solutions using digitonin to enhance fractionation according to Bronfman (Bronfman et al., 1998). Cells were centrifuged at 200*g* for 10 min, resuspended in 1.5 ml PBS, transferred to Eppendorf tubes, and centrifuged in a mini spin Eppendorf centrifuge operated at maximal speed (10,000*g*) for 30 s. The pellet was resuspended in 600 μl buffer A (0.25 M sucrose and 3 mM imidazole, pH 7.4) containing 1 mg/ml digitonin, and immediately centrifuged at maximal speed for 30 s. The pellet was again resuspended in 600 μl buffer A and transferred to a Dounce homogenizer. After 6 passes, the suspension was transferred into Eppendorf tubes and centrifuged at maximal speed for 30 s. The supernatant containing the cytoplasmic fraction was used for lipid extraction. The pellet containing the nuclear fraction was resuspended in 600 μl H_2O for lipid extraction.

To assess the presence of nuclear membranes and the quality of the isolation procedure, the nuclear fraction was controlled by electron microscopy (Fig. 1A) employing a conventional fixation protocol including fixation with 2.5% glutaraldehyde in 0.1 M NaK phosphate, pH 7.4, at 4 °C for 1 h, postfixation with 1% osmium

tetroxide in 0.1 M Na/K-phosphate, pH 7.4, at 4 °C, dehydration in a graded series of ethanol followed by 2 changes in acetone, and embedded in Epon followed by polymerization at 60 °C for 2.5 days. Sections of 50–60 nm thickness were stained with uranyl acetate and lead citrate, and analyzed in a TEM (Philips CM12) equipped with a slow-scan CCD camera (Gatan, Pleasanton, CA, USA) at an acceleration voltage of 100 kV. To control the cytoplasmic fraction and the purified virus, aliquots were used for negative staining with Na-phosphotungstic acid, pH 7.0, as described above, and examined in a Philips CM12 electron microscope.

Lipid extraction for determination of radioactivity

Lipids were extracted at room temperature according to the procedure described by Bligh and Dyer (Bligh, 1959). 500 µl chloroform and 1 ml methanol were added to 300 µl of suspensions (nuclear fraction, cytoplasmic fraction or virus) in glass tubes, vortexed 4 times within 10 min, and kept at room temperature for at least 30 min. After adding 500 µl chloroform and vortexing for 1 min, 500 µl of distilled water was added, the sample vortexed again for 1 min, and then centrifuged at 800*g* for 10 min to separate the lipid containing solvent phase from the aqueous phase. The solvent phase was collected in Eppendorf tubes that were placed on a warm plate (40 °C) in a safety hood for evaporation. Lipids were dissolved in 50 µl chloroform/methanol (4:1) immediately prior to using 5 µl aliquots for scintillation counting (LS 6500, Beckman Coulter Fullerton, CA, USA) according to the recommendation of the manufacturer.

Cryo-fixation for transmission electron microscopy

Cells grown on sapphire disks placed in 6-well-plates were frozen in a high-pressure freezing unit (HPM010; BAL-TEC, Balzers, Liechtenstein) as described in detail (Wild et al., 2001). The samples were then transferred to a freeze-substitution unit (FS 7500; Boeckeler Instruments, Tucson, Arizona) precooled to −88 °C for substitution with acetone and subsequent fixation with 0.25% glutaraldehyde and 0.5% osmium tetroxide rising the temperatures gradually to +2 °C to achieve good contrast of membranes. Cells were then embedded in Epon at 4 °C followed by polymerization at 60 °C for 2.5 days. Sections of 50–60 nm thickness were stained with uranyl acetate and lead citrate, and analyzed by TEM at an acceleration voltage of 100 kV.

Field emission scanning electron microscopy (FESEM)

Cells were grown for 2 days on cover slips of 10 mm in diameter (Mattek, Ashland, MA, USA) placed in 6-well-plates prior to inoculation. At 9, 12 or 16 hpi, 2.5% glutaraldehyde in 0.1 M Na/K-phosphate, pH 7.4, was added to the warm medium. Then dishes were kept at 4 °C for 1 h, medium replaced by 0.1 M Na/K-phosphate, and stored at 4 °C over night. Cells were post fixed with 1% osmium tetroxide in 0.1 M Na/K-Phosphate, pH 7.4, at 4 °C, critical point dried (BAL-TEC, CPD 030, Balzers, Liechtenstein), coated with 5 nm gold in a high vacuum sputtering device, (BAL-TEC SCD500), and examined in a FESEM (Supra 50 VP, Zeiss, Oberkochen, Germany) at an acceleration voltage of 3 kV using the inlens secondary electron detector.

Cryo-field emission scanning electron microscopy (Cryo-FESEM)

HSV-1 infected and mock infected cells grown in cell culture flasks were trypsinized and centrifuged at 150*g* for 8 min and prepared for examination in the frozen hydrated state as described (Wild et al., 2009). In brief, pellets were resuspended in fresh medium, fixed with 0.25% glutaraldehyde medium for 30 min at room temperature, and subsequently frozen – between two flat aluminum specimen carriers (scraped surfaces) with a TEM grid (12 µm) as a spacer – in a high-pressure freezing machine HPM010 (BAL-TEC). The frozen specimens were fractured in a freeze-fracturing device BAF 060 (BAL-TEC) at −120 °C and about 10^{-7} mbar, and, after partial freeze-drying ("etching") at −105 °C for 2 min, coated with platinum/carbon by electron beam evaporation. Then, specimen were transferred under high vacuum onto the cryo-stage in the SEM (LEO Gemini 1530, Zeiss, Oberkochen, Germany) for imaging at –115 °C and 5×10^{-7} mbar at an acceleration voltage of 5 kV using the inlens secondary electron detector.

Confocal microscopy

Cells were grown for 2 days on cover slips of 12 mm in diameter (Assistent, Sondheim, Germany). Then cells were infected with HSV-1 at a MOI of 5 and incubated at 37 °C for 9, 12 or 16 h. After fixation with 2% formaldehyde for 25 min at room temperature, the cells were permeabilized with 0.1% Triton-X-100 at room temperature for 7 min and blocked with 3% bovine serum albumin in phosphate-buffered saline (PBS) containing 0.05% Tween (PBST). To ascertain infectivity, cells were labeled with antibodies against the tegument protein VP16 (gift from B. Roizman, Chicago; USA) at a dilution of 1:1000 in PBST followed by a secondary anti-rabbit antibody (Alexa594; Invitrogen, Basel, Switzerland) at a dilution of 1:500 in PBST. After staining nuclei with DAPI, cells were embedded in glycergel containing 1,4-diazabicyclo[2.2.2]octane (DakoCytomation, Glostrup, Denmark) and analyzed using a confocal laser scanning microscope (SP2, Leica, Wetzlar, Germany).

Morphometric analysis

Nuclei of Vero cells are triaxial ellipsoids. Therefore, the absolute mean nuclear volume (V_n) and the absolute mean nuclear surface area (S_n) were calculated on the basis of the half axes (a, b, c) measured in 25 DAPI stained nuclei after deconvolution of confocal images according to the equations

$$V = \frac{4}{3}\pi abc \text{ and } S = 2\pi c^2 + 2\pi ab \int_0^1 \frac{1-u^2v^2x^2}{\sqrt{1-u^2x^2}\sqrt{1-v^2x^2}}dx$$

$$\text{where by } u = \frac{\sqrt{a^2-c^2}}{a} \text{ and } v = \frac{\sqrt{b^2-c^2}}{b}$$

On the basis of the absolute mean nuclear volume, the absolute mean cell volume can be evaluated by electron microscopic morphometric analysis of thin sections. For this, 20 images were sampled at random per experiment on cryo-fixed cells of 5 independent experiments at a final magnification of 6300×. From these images nuclear density (Vv_n) and cytoplasmic density (Vv_{cy}) were estimated applying the point counting method (Weibel, 1979) according to the equations $Vv_n = P_n/(P_n + P_{cy})$ and $Vv_{cy} = P_{cy}/(P_n + P_{cy})$, whereby P_n are points hitting the nucleus, and P_{cy} are points hitting the cytoplasm. On the basis of the absolute nuclear volume obtained from confocal images, the absolute mean cell volume (V_c) was calculated as $V_c = V_n/Vv_n$. The volume of discoid-like structures can easily be overestimated by point counting on thin sections. In order to get an idea of the cell volume to be expected, the mean area (F_c) occupied by cells grown on cover slips was measured on FESEM images using the Analysis Five software (Olympus, Hamburg, Germany). Assuming cells are cone-shaped with a central height (h) of 10 µm the mean volume was calculated taking the measured area F_c as base of the cones according to the equation $V_c = F_c \times h/3$.

Knowing the absolute cell volume, the surface area of cell organelles can be calculated and expressed in absolute values per mean cell volume. To determine the surface area of membrane compartments including INM, ONM, RER, Golgi complex and vacuoles containing virions, images of cryo-fixed cells were collected at random by TEM at a final magnification of 57,300 × from cells of 5 independent experiments. On these images the length of membranes was measured applying the point counting method using a multi purpose test system with 180 test points P and a test line length d corresponding to 182 nm at this given magnification. From these data, the surface density of the INM (Sv_i) and ONM (Sv_o) was calculated using the equations $Sv_{i,o}=4I_{i,o}/dP_n$, whereby $I_{i,o}$ are the number of intersections of the test lines d with the INM and ONM, respectively, and P_n the number of point hitting the nucleus. Then the absolute area of the nuclear membrane folds was calculated per mean nuclear volume: $S_i=Sv_i \times V_n$ and $S_{o,}=Sv_o \times V_n$. Similarly, the length of cytoplasmic membranes was measured, and the surface density of the RER (Sv_r) Golgi complex (Sv_g) and vacuoles containing virions (Sv_v) was estimated according the equation $Sv_{r,g,v}=I_{r,g,v}/dP_{cy}$, whereby $I_{r,g,v}$ are intersections of the test lines with RER, Golgi or vacuolar membranes, and P_{cy} are points hitting the cytoplasm. The mean surface area of RER (S_r) of Golgi complex (S_g) and of vacuoles (S_v) was calculated per mean cell volume: $S_{r,g,v}=Sv_{r,g,v} \times Vv_{cy} \times V_c$.

Phenotype distribution

The presence of virus particles in thin sections for TEM is very irregular depending on the onset of infection and the section plane. To estimate distribution of virus particles, 25 cell profiles were selected at random at each time point, virus particles counted and expressed as mean number per cell profile.

Endocytosis assay

Fluid-phase endocytosis was measured according to (Steinman et al., 1974). Cells were grown in 6-well-plates for 48 h prior to inoculation. After 5, 9, 12 and 16 h medium was replaced by DMEM containing 1 mg/ml horse radish peroxidase (HRP; Sigma-Aldrich, Buchs, Switzerland) and cells were incubated at 37 °C for 30 min. Cells were then washed 5 times for 4 min with DMEM, incubated in DMEM supplemented with 5% FCS at 37 °C for 30 min and rinsed twice in PBS. One ml of 0.05% Triton X-100 was added and cells were kept on ice for 10 min. Cells were scraped and homogenized by repetitive pipetting (20 times). HRP enzymatic activity was assayed at 460 nm after 15 min of reaction time using 0.342 mM O-dianisidine dihydrochloride (Acros Organics, Geel, Belgium) and 0.003% H_2O_2 in 0.5 M Na-phosphate, pH 5.0, containing 0.3% Triton X-100 as substrate. Data were normalized to the actual cell number.

Determination of mitotic activity

Cells were seeded on glass cover slips (Assistent) placed in 6-well-plates at a density of 5×10^5 cells per well. After 48 h the cells were infected with HSV-1 at MOI of 5 or mock-infected. After 0, 3, 6, 9 or 12 h of incubation cells were washed briefly with PBS, fixed with 2% formaldehyde for 30 min at room temperature, and washed briefly with PBS. Nuclei were stained with 4′,6-diamidino-2-phenylindole (DAPI). Cells were embedded in fluorescence mounting medium (DakoCytomation, Glostrup, Denmark) on glass slides. Nuclei were counted under a fluorescence microscope, and the percentage of cells in anaphase and metaphase was determined.

Statistical analysis

Mean and standard deviation of [^{3}H]-choline uptake, morphometric data and endocytosis assays were calculated and compared by a multiple t test using the software GraphPad Prism 3.

Acknowledgments

The authors wish to thank B. Roizman, University of Chicago, for antibodies, Elisabeth Högger-Manser and Mirela Vitanescu for technical advice and support. The study was supported by the Foundation for Scientific Research at the University of Zürich.

References

Asher, Y., Heller, M., Becker, Y., 1969. Incorporation of lipids into herpes simplex virus particles. J. Gen. Virol. 4 (1), 65–76.
Ben-Porat, T., Kaplan, A.S., 1971. Phospholipid metabolism of herpesvirus-infected and uninfected rabbit kidney cells. Virology 45 (1), 252–264.
Ben-Porat, T., Kaplan, A.S., 1972. Studies on the biogenesis of herpesvirus envelope. Nature 235 (5334), 165–166.
Bligh, 1959. A rapid method of total lipid extraction and purification. Can. J. Biochem. Physiol. 37 (8), 911–917.
Borchers, K., Oezel, M., 1993. Simian Agent 8 (SA8): morphogenesis and ultrastructure. Zentralbl. Bakteriol. 279, 526–536.
Bronfman, M., Loyola, G., Koenig, C.S., 1998. Isolation of intact organelles by differential centrifugation of digitonin-treated hepatocytes using a table eppendorf centrifuge. Analyt. Biochem. 255 (2), 252–256.
Campadelli-Fiume, G., Farabegoli, F., Di Gaeta, S., Roizman, B., 1991. Origin of unenveloped capsids in the cytoplasm of cells infected with herpes simplex virus 1. J. Virol. 65 (3), 1589–1595.
Daniel, L.W., Waite, M., Kucera, L.S., King, L., Edwards, I., 1981. Phospholipid synthesis in human embryo fibroblasts infected with herpes simplex virus type 2. Lipids 16 (9), 655–662.
Darlington, R.W., Moss, L.H., 1968. Herpesvirus envelopment. J. Virol. 2 (1), 48–55.
de Bruyn Kops, A., Knipe, D.M., 1988. Formation of DNA replication structures in herpes virus-infected cells requires a viral DNA binding protein. Cell 55 (5), 857–868.
Ehmann, G.L., McLean, T.I., Bachenheimer, S.L., 2000. Herpes simplex virus type 1 infection imposes a G(1)/S block in asynchronously growing cells and prevents G(1) entry in quiescent cells. Virology 267 (2), 335–349.
Farnsworth, A., Wisner, T.W., Webb, M., Roller, R., Cohen, G., Eisenberg, R., Johnson, D.C., 2007. Herpes simplex virus glycoproteins gB and gH function in fusion between the virion envelope and the outer nuclear membrane. Proc. Natl. Acad. Sci. USA 104 (24), 10187–10192.
Gilbert, R., Ghosh, K., Rasile, L., Ghosh, H.P., 1994. Membrane anchoring domain of herpes simplex virus glycoprotein gB is sufficient for nuclear envelope localization. J. Virol. 68 (4), 2272–2285.
Goldberg, M.W., Allen, T.D., 1995. Structural and functional organization of the nuclear envelope. Cur. Opi. Cell Biol. 7 (3), 301–309.
Granzow, H., 2001. Egress of alphaherpesviruses: comparative ultrastructural study. J. Virol. 75 (8), 3675–3684.
Granzow, H., Weiland, F., Jons, A., Klupp, B.G., Karger, A., Mettenleiter, T.C., 1997. Ultrastructural analysis of the replication cycle of pseudorabies virus in cell culture: a reassessment. J. Virol. 71 (3), 2072–2082.
Grunewald, K., Desai, P., Winkler, D.C., Heymann, J.B., Belnap, D.M., Baumeister, W., Steven, A.C., 2003. Three-dimensional structure of herpes simplex virus from cryo-electron tomography. Science 302 (5649), 1396–1398.
Henneberry, A.L., Wright, M.M., McMaster, C.R., 2002. The major sites of cellular phospholipid synthesis and molecular determinants of fatty acid and lipid head group specificity. Mol. Biol. Cell 13 (9), 3148–3161.
Hess, M.W., Muller, M., Debbage, P.L., Vetterlein, M., Pavelka, M., 2000. Cryopreparation provides new insight into the effects of brefeldin A on the structure of the HepG2 Golgi apparatus. J. Struct. Biol. 130 (1), 63–72.
Homman-Loudiyi, M., Hultenby, K., Britt, W., Soderberg-Naucler, C. (2003). Envelopment of human cytomegalovirus occurs by budding into Golgi-derived vacuole compartments positive for gB, Rab 3, trans-golgi network 46, and mannosidase II. [erratum appears in J. Virol. Arch. 2003 Jul;77(14):8179]. J. Virol. 77 (5), 3191–203.
Jackowski, S., 1994. Coordination of membrane phospholipid synthesis with the cell cycle. J. Biol. Chem. 269 (5), 3858–3867.
Jackowski, S., 1996. Cell cycle regulation of membrane phospholipid metabolism. J. Biol. Chem. 271 (34), 20219–20222.
Klupp, B.G., Granzow, H., Mettenleiter, T.C., 2011. Nuclear envelope breakdown can substitute for primary envelopment-mediated nuclear egress of herpesviruses. J. Virol. 85 (16), 8285–8292.
Kucerka, N., Tristram-Nagle, S., Nagle, J.F., 2006. Closer look at structure of fully hydrated fluid phase DPPC bilayers. Biophys. J. 90 (11), L83–L85.
Laue, M., Piesker, J., Bannert, N., 2009. Detection limit in diagnostic electron microscopy of model suaspensions. Microsc. Con., Graz, Austria 2, 435–436.

Leuzinger, H., Ziegler, U., Schraner, E.M., Fraefel, C., Glauser, D.L., Heid, I., Ackermann, M., Mueller, M., Wild, P., 2005. Herpes simplex virus 1 envelopment follows two diverse pathways. J. Virol. 79 (20), 13047–13059.
Lim, R.Y., Fahrenkrog, B., 2006. The nuclear pore complex up close. Cur. Opin. Cell Biol. 18 (3), 342–347.
Maul, 1977. The nuclear and cytoplasmic pore complex. Structure, dynamics, distribution and evolution. Int. Rev. Cytol. Suppl. 6, 75–186.
Mettenleiter, T.C., 2004. Budding events in herpesvirus morphogenesis. Virus Res. 106 (2), 167–180.
Mettenleiter, T.C., Klupp, B.G., Granzow, H., 2006. Herpesvirus assembly: a tale of two membranes. Cur. Opin. Microbiol. 9 (4), 423–429.
Monier, K., Armas, J.C., Etteldorf, S., Ghazal, P., Sullivan, K.F., 2000. Annexation of the interchromosomal space during viral infection. Nature Cell Biol. 2 (9), 661–665.
Nii, S., Morgan, C., Rose, H.M., 1968. Electron microscopy of herpes simplex virus. II. Sequence of development. J. Virol. 2 (5), 517–536.
Orci, L., Montesano, R., Perrelet, A., 1981. Exocytosis-endocytosis as seen with morphological probes of membrane organization. Meth. Cell Biol. 23, 283–300.
Palade, G., 1975. Intracellular aspects of the process of protein synthesis. Science 189 (4200), 347–358.
Poon, A.P., Benetti, L., Roizman, B., 2006. U(S)3 and U(S)3.5 protein kinases of herpes simplex virus 1 differ with respect to their functions in blocking apoptosis and in virion maturation and egress. J. Virol. 80 (8), 3752–3764.
Radsak, K., Eickmann, M., Mockenhaupt, T., Bogner, E., Kern, H., Eis-Hubinger, A., Reschke, M., 1996. Retrieval of human cytomegalovirus glycoprotein B from the infected cell surface for virus envelopment. Arch. Virol. 141 (3-4), 557–572.
Reynolds, A.E., Wills, E.G., Roller, R.J., Ryckman, B.J., Baines, J.D., 2002. Ultrastructural localization of the herpes simplex virus type 1 UL31, UL34, and US3 proteins suggests specific roles in primary envelopment and egress of nucleocapsids. J. Virol. 76 (17), 8939–8952.
Roizman, B., Knipe, D.M., 2001. Herpes simplex viruses and their replication. 4th ed. In: K. D M, Howly, P.M. (Eds.), Fields Virology, 2. Lipincott-Raven Publishers, Philadelphia, pp. 2399–2460.
Roizman, B., Knipe, D.M., Whiley, R.J., 2007. Herpes simplex viruses. 5th ed. In: K. D M, Howly, P.M. (Eds.), Fields Virology, Vol. 2. Lipincott-Raven Publishers, Philadelphia, pp. 2501–2601. 2 vols.
Schwartz, J., Roizman, B., 1969. Concerning the egress of herpes simplex virus from infected cells: electron and light microscope observations. Virology 38 (1), 42–49.
Simpson-Holley, M., 2005. Identification and functional evaluation of cellular and viral factors involved in the alteration of nuclear architecture during herpes simplex virus 1 infection. J. Virol. 79 (20), 12840–12851.
Simpson-Holley, M., Colgrove, R.C., Nalepa, G., Harper, J.W., Knipe, D.M., 2005. Identification and functional evaluation of cellular and viral factors involved in the alteration of nuclear architecture during herpes simplex virus 1 infection. J. Virol. 79 (20), 12840–12851.
Skepper, J.N., Whiteley, A., Browne, H., Minson, A., 2001. Herpes simplex virus nucleocapsids mature to progeny virions by an envelopment—deenvelopment–reenvelopment pathway. J. Virol. 75 (12), 5697–5702.
Stackpole, C.W., 1969. Herpes-type virus of the frog renal adenocarcinoma. I. Virus development in tumor transplants maintained at low temperature. J. Virol. 4 (1), 75–93.
Stannard, L.M., Himmelhoch, S., Wynchank, S., 1996. Intra-nuclear localization of two envelope proteins, gB and gD, of herpes simplex virus. Arch. Virol. 141 (3-4), 505–524.
Steinhart, W.L., Nicolet, C.M., Howland, J.L., 1981. Incorporation of 32P-phosphate into membrane phospholipids during infection of cultured human fibroblasts by herpes simplex virus type 1. Intervirology 16 (2), 80–85.
Steinman, R.M., Silver, J.M., Cohn, Z.A., 1974. Pinocytosis in fibroblasts. Quantitative studies in vitro. J. Cell Biol. 63 (3), 949–969.
Torrisi, M.R., Di Lazzaro, C., Pavan, A., Pereira, L., Campadelli-Fiume, G., 1992. Herpes simplex virus envelopment and maturation studied by fracture label. J. Virol. 66 (1), 554–561.
van Genderen, I.L., Godeke, G.J., Rottier, P.J., van Meer, G., 1995. The phospholipid composition of enveloped viruses depends on the intracellular membrane through which they bud. Biochem. Soc. Trans. 23 (3), 523–526.
van Meer, G., Voelker, D.R., Feigenson, G.W., 2008. Membrane lipids: where they are and how they behave. Nat. Rev. Mol. Cell Biol. 9 (2), 112–124.
Weibel, E., 1979. Stereological Methods. Practical Methods for Biological Morphometry, Vol. 1. Academic Press, London.
Weibull, C., Villiger, W., Carlemalm, E., 1984. Extraction of lipids during freeze-substitution of Acholeplasma laidlawii-cells for electron microscopy. J. Microsc. 134 (2), 213–216.
Whealy, M.E., Card, J.P., Meade, R.P., Robbins, A.K., Enquist, L.W., 1991. Effect of brefeldin A on alphaherpesvirus membrane protein glycosylation and virus egress. J. Virol. 65 (3), 1066–1081.
Wild, P., (2008). Electron microscopy of viruses and virus-cell interactions. T.Allen. In: Introduction to Electron Microscopy for Biologists. Meth. Cell Biol., Elsevier, vol. 88, pp. 497–524.
Wild, P., Gloor, S., Vetsch, E., 1985. Quantitative aspects of membrane behavior in rat parathyroid cells after depression or elevation of serum calcium. Lab. Invest. 52 (5), 490–496.
Wild, P., Schraner, E.M., Adler, H., Humbel, B.M., 2001. Enhanced resolution of membranes in cultured cells by cryoimmobilization and freeze-substitution. Microsc. Res. Tech. 53 (4), 313–321.
Wild, P., Schraner, E.M., Cantieni, D., Loepfe, E., Walther, P., Muller, M., Engels, M., 2002. The significance of the Golgi complex in envelopment of bovine herpesvirus 1 (BHV-1) as revealed by cryobased electron microscopy. Micron 33 (4), 327–337.
Wild, P., Senn, C., Manera, C.L., Sutter, E., Schraner, E.M., Tobler, K., Ackermann, M., Ziegler, U., Lucas, M.S., Kaech, A., 2009. Exploring the nuclear envelope of herpes simplex virus 1-infected cells by high-resolution microscopy. J. Virol. 83 (1), 408–419.
Wisner, T.W., Wright, C.C., Kato, A., Kawaguchi, Y., Mou, F., Baines, J.D., Roller, R.J., Johnson, D.C., 2009. Herpesvirus gB-induced fusion between the virion envelope and outer nuclear membrane during virus egress is regulated by the viral US3 kinase. J. Virol. 83 (7), 3115–3126.